Research Article

Nanoparticles in toner material

M. Getzlaff[1] · M. Leifels[1] · P. Weber[1] · Ü. Kökcam-Demir[2] · Ch. Janiak[2]

Abstract
Printer toner is a material in everyday life. It is a cheap material which is distributed by many companies. Each printer and copier require specific toner material. Therefore, differences in the consistence occur concerning the size and chemical composition of the toner particles. They are known as microscaled objects which are made up of nanoparticles. The first goal of this investigation was to determine the material composition as well as the size, the shape and the possible crystallinity of the particles from three different toner materials (distributed by Hewlett-Packard, Lyreco and Epson) to turn one's attention whether these nanoparticles can be taken for scientific investigations instead of carrying out sophisticated preparation procedures. It was found that cheap toner material can be used to obtain crystalline SiO_2 nanoparticles with a size of about 10–20 nm using the investigated toner material from HP and Lyreco. With benzene as solvent, they are agglomerated to particles of about 200–400 nm. Using n-hexane one gets single nanoparticles without agglomeration. Additionally, amorphous carbon nanoparticles can be gained with a size of approximately 80 nm using the toner powder from Epson. A further goal was directed to give more information concerning possible health hazards due to the use of printers and copiers which emit particle dust coming from the toner. Due to that particulate pollution inspiration can result in inflammatory processes in the lung up to lung cancer. Additionally, nanoparticles can have a toxic effect within cells and be mutagenic. For all three toner materials, the particles without dissolving show a diameter of about 10 µm. Therefore, most of these particles should remain in the nasopharyngeal region without reaching the alveolar region.

Keywords Toner · Nanoparticles · Nanotoxicology · Inhalation

1 Introduction

Printer toner is a material in everyday life. It is a cheap material which is distributed by many companies. Each printer and copier require specific toner material. Therefore, differences in the consistence occur concerning the size and chemical composition of the toner particles. They are known as microscaled objects which are made up of nanoparticles [1].

Thus, the question arises whether these nanoparticles can be taken for scientific investigations instead of carrying out sophisticated preparation procedures as, e.g., in gas aggregation sources [2], arc cluster ion sources [3] or magnetron sources [4] which require vacuum (a detailed overview is given in [5]) with a subsequent size selection [6, 7] or by wet-chemical processes [8]. The great advantage would be a fast and cheap possibility to obtain specific nanoparticles. An additional option would be the potential to use them for teaching purpose as well as for practical training.

The first step into that direction must be directed toward the determination of the chemical composition of the nanoparticles in order to see which materials are offered.

For nanoscaled objects, every property depends significantly on the size [6], for example, optical [9–11], electronic [12], mechanical [6], chemical [13], magnetic properties [14] or the melting behavior [15].

✉ M. Getzlaff, getzlaff@uni-duesseldorf.de | [1]Institute of Applied Physics, University of Düsseldorf, 40225 Düsseldorf, Germany. [2]Institute of Inorganic and Structural Chemistry, University of Düsseldorf, 40225 Düsseldorf, Germany.

SN Applied Sciences (2019) 1:489 | https://doi.org/10.1007/s42452-019-0501-9

Received: 10 December 2018 / Accepted: 16 April 2019 / Published online: 25 April 2019

Therefore, it is extremely important to investigate not only the size but also the size distribution of the particles. The questions to be answered are related to whether a monomodal or multimodal distribution is present, the width of the distribution, the influence of different solvents on these properties and the distinction of toner material from different companies.

Such an investigation may also be helpful to give more information concerning possible health hazards due to the use of printers and copiers [16] which emit particle dust coming from the toner [17–20]. Due to that particulate pollution inspiration [21, 22] can result in inflammatory processes in the lung up to lung cancer [23–27]. The review of Bierkandt et al. [28] summarizes the toxicological effects of inhaled nanoparticles which have been already identified explaining the processes which cause different mechanisms in the respiratory tract and their resulting effects. Additionally, nanoparticles can have a toxic effect within cells and be mutagenic [29]. It was shown [30, 31] that this can be understood due to modification of the DNA methylation.

Unfortunately, only little quantitative information is available for the characterization concerning the size and chemical composition of the particulate matter emitted by office equipment [32, 33]. But, a toxicological assessment of the emitted particles requires the knowledge of their chemical composition [34]. Also, former investigations are carried out in dependence of printer or copier types [19] but not of possible toners which are made up of different content. The use of different toners may be the explanation why in investigations of printers not only from different manufacturers but also for identically constructed devices often significant differences in the behavior of emitted nanoparticles are present [35]. Additionally, this emission depends on the temperature of the fuser [36, 37] and on the blackening rate of the print-out [19]. A subsequent detailed investigation showed that not the absolute temperature of the fuser plays the dominant role but the temperature difference between the fuser and the environment [38].

The goal of this investigation is to determine the material composition as well as the size, the shape and the possible crystallinity of the particles using several respective methods.

An additional aspect is related to possible differences in toners which are distributed by original equipment manufacturers to be used exclusively in their own printers and toners from general office supplies manufacturers to be used in many printer types which often offer recycled toner material.

Scanning electron microscopy (SEM) allows to image the shape of metallic objects and therefore in the case of particles the size. For thin samples or small objects, the size can also be determined using transmission electron microscopy (TEM).

With the help of energy-dispersive X-ray spectroscopy (EDX), the toner material can be analyzed for the elements present. The X-rays emitted by the sample are characteristic of its element composition and may thus be used for qualitative and (semi)quantitative analysis. The generation of these characteristic X-rays can be carried out with X-rays as well as with high-energy electrons of, e.g., a scanning or transmission electron microscope.

In order to investigate properties of crystalline materials, X-ray diffraction (XRD) represents a powerful tool. A powder X-ray diffractometer allows to study polycrystalline samples. Taking the Bragg condition in combination with monochromatic X-rays the diffraction at different net planes makes the option available to evaluate a specific Bravais lattice of a single compound or a mixture of compounds. The parameters of the corresponding lattice are characteristic which thus enables to determine the element itself or the stoichiometry of alloys.

For particles in a solution, the size can be independently determined using dynamic light scattering (DLS) also known as photon correlation spectroscopy (PCS). The analysis of scattered laser light enables to determine the diffusion coefficient of particles. Particles of different size exhibit a different pronounced Brownian motion. Smaller particles possess a larger diffusion coefficient, larger ones a smaller coefficient. Using the Stokes–Einstein equation, it is subsequently possible to derive their size. Because particles in the solution have a ligand shell which influences the diffusion it is important to note that the size being evaluated using this method is thus not identical to the size coming from SEM and TEM measurements but is larger.

2 Experimental details

2.1 Experimental techniques

Dynamic light scattering (also known as photon correlation spectroscopy PCS) uses scattered monochromatic light of dispersed material in a liquid. This technique allows to determine the diffusion coefficient D of the particles. This parameter depends among others on their size:

$$D = \frac{kT}{3\pi\eta R} \tag{1}$$

with T the temperature, η the viscosity of the liquid and R the so-called hydrodynamic radius. Thus, it is possible to estimate the size of nanoparticles in the range of nanometers up to about several µm. The hydrodynamic radius is a measure for the force to translate the object "particle"

or molecule through the solvent. Therefore, it generally results in larger values as compared to the core because the ligand shell of the particle also plays a nonnegligible role.

With respect to the characterization of the particle's size distribution, a parameter used to define the size range of the particles in a solvent is called the "polydispersity index" (PDI). The term "polydispersity" (or "dispersity" as recommended by IUPAC) is used to describe the degree of nonuniformity of a size distribution of particles. PDI is a number calculated from a two-parameter fit to the correlation data being gained during the DLS measurement. This index is dimensionless and scaled such that values smaller than 0.05 are mainly obtained with highly monodisperse standards. PDI values bigger than 0.7 indicate that the sample has a very broad particle size distribution and is probably not suitable to be analyzed by the dynamic light scattering technique.

X-ray diffraction (XRD) allows to identify unknown material if it is crystalline which bases on the Bragg condition. One specific version of XRD is powder diffractometry which enables to investigate even polycrystalline samples. In this case, monochromatic X-rays illuminate the material under the varying angle θ with the detector being rotatable under 2θ. Intensity peaks due to diffraction at specific values of 2θ allow to calculate the distance between net planes and the respective Miller indices which are fingerprints of each crystalline material. The subsequent use of databases containing lots of diffraction pattern enables the determination of all contemplable species.

The size of nanoscaled objects like nanoparticles can additionally be estimated using the width of each diffraction peak with θ the Bragg angle. This relation is known as the Scherrer [39] equation:

$$d = \frac{K \cdot \lambda}{w \cdot \cos\theta} \tag{2}$$

with d the diameter of the nanoscaled object, K the Scherrer constant, λ the wavelength of the X-rays and w the width (e.g., the full width at half maximum FWHM). It should be noted that w is given in rad, for values in degree a proportionality factor of 57.3 must be taken into account.

Transmission electron microscopy (TEM) is used to determine the size of the particles. Because the absorption scales with the atomic number their metallic core can be distinguished from the solvent shell which mainly consists of light elements like C. Only thin systems or small particles can be investigated due to the transmission of the electron beam through the sample. The focused electron beam also results in the emission of characteristic X-rays. Their energy depends on the difference of electron binding energies. Therefore, this additionally carried out technique (*energy-dispersive X-ray spectroscopy* EDX) allows to determine the chemical composition with the same resolution as the TEM investigation itself.

Scanning electron microscopy (SEM) uses reflected electrons. Thus, the restriction to thin samples or small particles in a TEM investigation is not given. The electron energy is lower as in TEM which results in a reduced lateral resolution. The electrons can also be used for EDX in order to determine the chemical composition. It should be noted that for light elements up to about $Z = 9$ the quantification of the relative amount cannot be given with high accuracy. Therefore, these values are only discussed in the following in a qualitative way.

2.2 Technical equipment

For XRD measurements, the D2 Phaser from Bruker was used which has a power of 300 W (30 kV, 10 mA) and a photon energy of 8.04 keV (Cu K_α, $\lambda = 1.5418$ Å) with a flat Silicon, low background sample holder. DLS investigations were carried out with the Nano S Zetasizer from Malvern. It allows to determine particle sizes between 0.3 and 1000 nm, exhibits a laser wavelength of 633 nm and measures the scattered light under an angle of 173°. The TEM is the type E902 from Zeiss and allows a magnification up to about 150,000. The HR-TEM is the model JEM-ARM200F from JEOL with the additional option to do EDX investigations. The SEM type JSM6510LVQSEM from JEOL is equipped with a LaB_6 cathode at 5–20 keV and a detector for EDX being Silicon-Drift-Detector x-Flash 410 from Bruker.

2.3 Types of different toners

The toner from the company Lyreco (type 4.563.182) can be used for HP printers of the 2000 series and for Canon printers of the LBP 6000 and MF 5000 series. The toner HP CE320A from Hewlett-Packard with code number 128A is manufactured for the HP LaserJet and HP LaserJet Pro series. The toner from Epson with the article number C 13 SO 50005-K is used for the printer series EPL 5500.

2.4 Sample preparation

The toner particles were extracted directly from the fill (printer toner) of the respective cartridge by using a metallic powder spatula. Subsequently, they were filled into closed plastic tubes to be stored and used for the following measurements.

For the investigations with SEM/EDX and XRD, the respective printer toner with the nanoparticles from the closed plastic tube was put directly into the measurement devices without adding any solvent.

(a) *SEM* Depending on the conductivity some samples have to be covered with gold (like the printer toner of Epson). If a sample exhibits a high conductivity (like the printer toner of Lyreco), it does not have to be covered with gold. Each sample was applied to the brass and aluminum holder of the SEM. Therefore, the signals from Au, Al, Cu and Zn in EDX measurements were neglected because these elements are not present in the original toner material.
(b) *XRD* The undissolved sample was directly put into the diffractometer.

For DLS and TEM/EDX measurements a rolled edge glass (Behr Labor-Technik GmbH; 20 ml) was filled with a small amount of the respective printer toner. Subsequently, a solvent (benzene or n-hexane) was given to the printer toner until the whole dissolved sample became transparent with a possible subsequent dispersion of the nanoparticles.

(c) *DLS* With the help of a glass Pasteur pipette (Brand GmbH+Co KG; 2 ml), the dissolved sample was dripped into a glass cuvette which was covered with a cap in order to prevent to get rid of the solvent.
(d) *TEM* A drop of the dissolved sample was given on a copper grid (Plano GmbH; Formvar/Carbon film; 200 mesh) using a glass Pasteur pipette.

3 Results

In this section, the properties of three different toner materials will be presented in detail. Two toner powders are from original equipment manufacturers (Hewlett-Packard and Epson) to be used exclusively in their own printers and, for comparison, one from Lyreco being a general office supplies manufacturer to be used in many different printer types. These results are discussed and compared in the subsequent Sect. 4 concerning the different aspects given above.

3.1 Toner Hewlett-Packard

The content can be found in the data sheet to be amorphous silica, carbon black, styrene acrylate copolymer and wax. The respective relative amount is not declared.

3.1.1 EDX

The chemical composition was determined by EDX and is listed in Table 1.

All detected elements are part of the components stated in the data sheet and no one is missing.

Table 1 Chemical composition of the HP CE320A toner material obtained by EDX

Element	At. weight (%)	Uncertainty (%)
C	97.2	10.6
O	2.2	0.6
Si	0.6	0.1

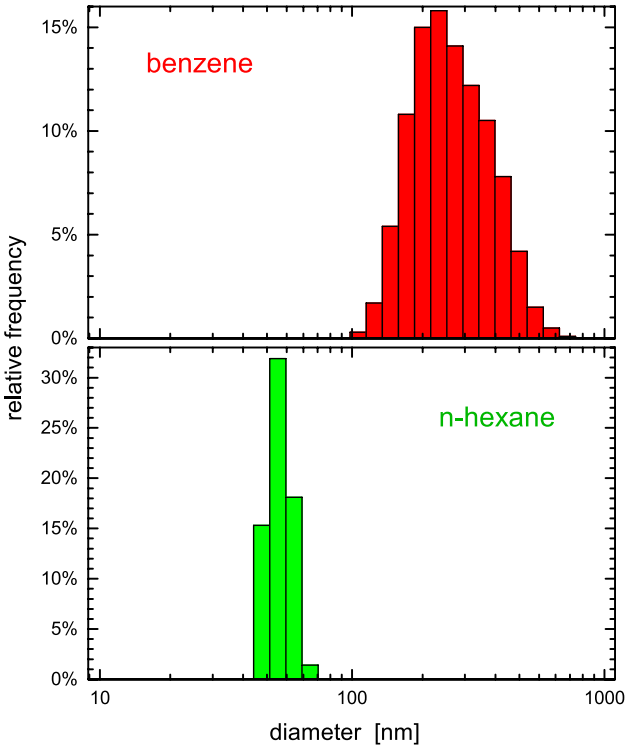

Fig. 1 Hydrodynamic diameter of HP CE320A toner material obtained by DLS. Top: dissolved in benzene. Bottom: dissolved in n-hexane

3.1.2 DLS

After dissolving the toner material in benzene large particles with hydrodynamic diameters between 100 and 700 nm are present (see top part of Fig. 1). The polydispersity index of 0.34 points to a moderately polydisperse size distribution. Using n-hexane as solvent one obtains significantly smaller particles (see bottom part of Fig. 1) which points to the subsequent dispersion of the nanoparticles in the solvent. Their hydrodynamic diameters are between 40 and 70 nm.

3.1.3 XRD

For the determination of the crystallinity of the nanoparticles in the toner material, X-ray diffraction measurements

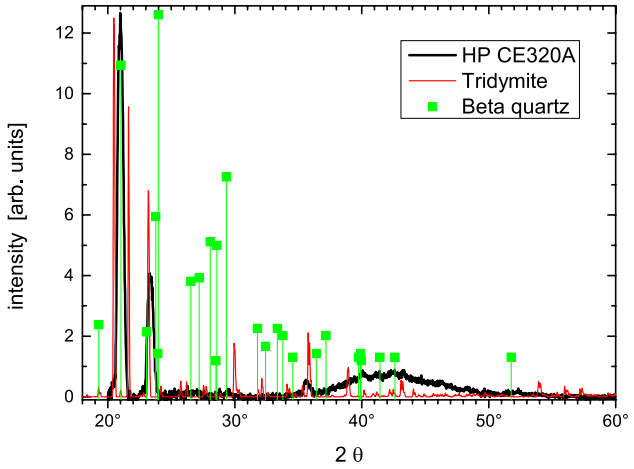

Fig. 2 X-ray diffraction pattern of the HP CE320A toner material after background subtraction (black curve). Two reference diffractograms were additionally given with tridymite (red curve) and β -quartz (green dots) scaled to obtain the same maximum value

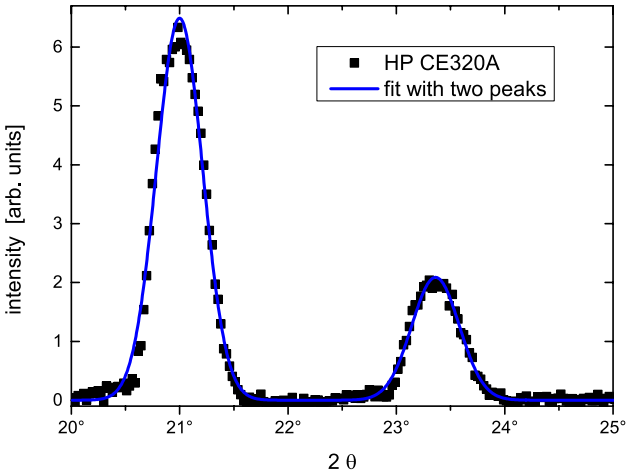

Fig. 3 X-ray diffraction pattern of HP CE320A toner material in the angle range between 20° and 25° (black dots). Both peaks were fitted with two Gaussian functions (blue line)

were carried out (see Fig. 2). The black curve shows the diffraction intensity of the toner material. The only materials which exhibit nearly the same diffraction peaks and are also made up of the elements which were determined by EDX (C, Si, O) are tridymite and β-quartz. The respective diffraction patterns are additionally given in Fig. 2. The red curve shows the pattern of tridymite, and the values were obtained from the RRUFF database (R090042). The green dots are values of β- or high-quartz [40] both being made up of silica.

One alone cannot reproduce all pattern of the toner. The pattern at about 21° agrees with one of β-quartz, whereas tridymite exhibits two peaks at 20.5° and 21.5°. The peak at 23° can be reproduced with both materials. At higher angles, no additional sharp peaks occur. Therefore, the diffraction pattern hints to crystalline particles consisting of both types of silica. The broad structure between 38° and 48° can be understood as being due to amorphous carbon.

The two peaks of the diffraction pattern with the highest intensity are taken to estimate the size of the crystalline particles using the Scherrer equation (see Eq. 2). The black dots represent the measurement of the toner material, the blue curve a fit with two Gaussian functions (see Fig. 3) which can reproduce the data very well. The fit results in an angle of $(21.0 \pm 0.1)°$ and a width (FWHM) of $(0.50 \pm 0.01)°$ for the first peak and an angle of $(23.4 \pm 0.1)°$ and a width of $(0.52 \pm 0.02)°$ for the second peak, resp. Using a Scherrer constant K of 0.94 which is taken for spherical particles with cubic symmetry, the obtained diameters amount to (16.9 ± 0.3) nm for the first and (16.3 ± 0.7) nm for the second peak.

3.1.4 TEM

TEM images of the toner material which was dissolved in benzene are presented in Fig. 4. The left image shows large agglomerates with sizes of several 100 nm. A more detailed view is given in the right image. The object in the upper area proves that the agglomerates consist of small particles with sizes of about 20 nm. EDX measurements carried out with high-resolution TEM show that only the chemical elements Si, C and O are present in the nanoparticles.

3.1.5 SEM

SEM was used to investigate the toner material without (previous) dissolving (see Fig. 5). The left part shows large and nearly spherical particles with sizes between about 5 µm and 10 µm. Using a high magnification (right part), the respective surfaces can be imaged. It is obvious that a lot of particles are located on the surface which are significantly smaller than 50 nm.

3.1.6 Conclusion

The determination of the chemical composition by EDX/SEM results in C, Si and O and confirms the specification of the data sheet. The EDX measurement in a high-resolution TEM proves that the observed nanoparticles consist of these elements.

These results are in agreement with XRD investigations which demonstrate that crystalline material is present which is exclusively made up of silica. The observed

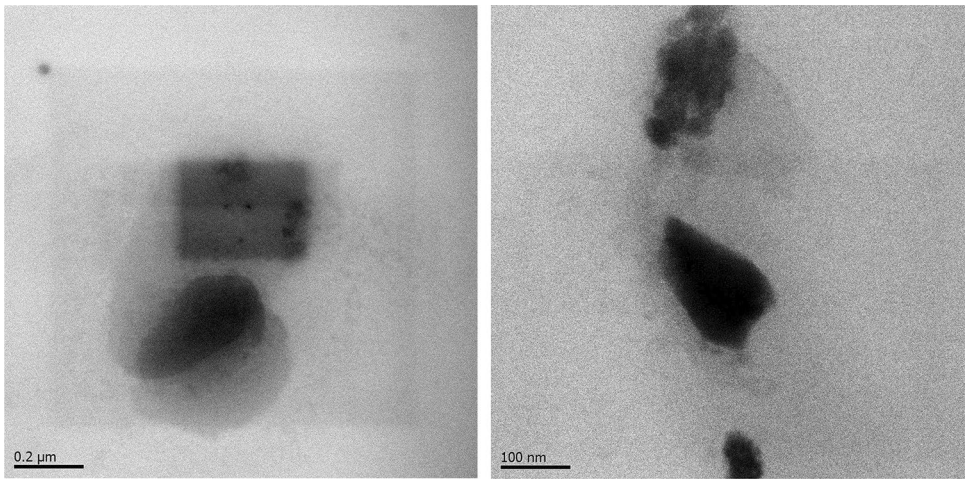

Fig. 4 TEM image of HP CE320A toner material dissolved in benzene. Left: scale bar: 200 nm. Right: scale bar: 100 nm

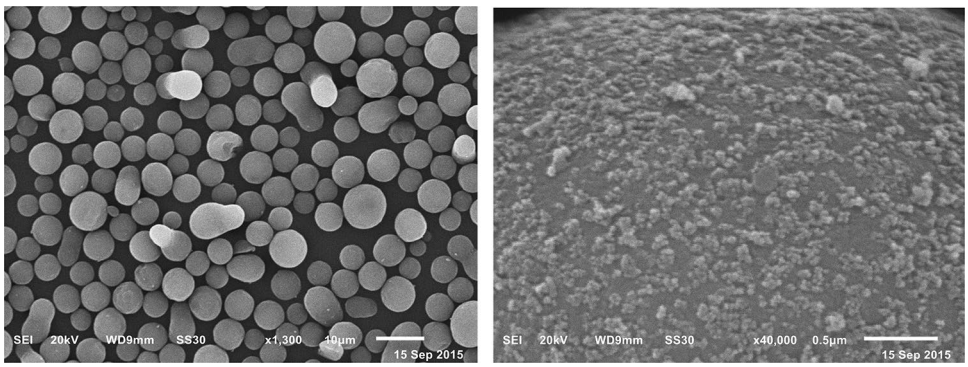

Fig. 5 SEM images of the HP CE320A toner material without a previous dissolving. Left: scale bar: 10 µm. Right: scale bar: 500 nm

patterns can be understood by the coexistence of the two high-temperature configurations tridymite and β-quartz.

The SEM measurements show that the toner powder is build up of large particles with a size of about 10 µm which exhibit nanoparticles on their surface with a diameter below 50 nm. In a solution, these large particles are not observable. This points to that they can be build up of, e.g., copolymers which are dissolved in the respective solvent. Subsequently, the nanoparticles from the surface are also dissolved. This was proven using DLS which led to different hydrodynamic diameters after dissolving in benzene with 250 nm and in n-hexane with about 60 nm. An additional confirmation was given in the TEM investigation which showed larger particles with diameters of several 100 nm being made up of smaller ones with a size of about 20 nm. These small nanoparticles represent the crystalline material in the toner which was proven by the width of the XRD diffraction peaks. Using the Scherrer equation results in a diameter of about 20 nm.

3.2 Toner Epson

A data sheet declaring the content of the toner material is not available.

Table 2 Chemical composition of the Epson toner

Element	At. weight (%)	Uncertainty (%)
C	89.4	5.4
O	9.7	1.1
Other	0.9	

3.2.1 EDX

The composition of this toner is given in Table 2. In contrast to the other ones discussed only C and O are present but neither metals nor relevant amount of Si. It is therefore most likely that the material exclusively consists of polymers.

3.2.2 DLS

The toner material was dissolved in benzene as well as in n-hexane. The respective hydrodynamic diameters were determined using DLS (see Fig. 6). The mean diameter of the particles being dissolved in benzene is about 200 nm

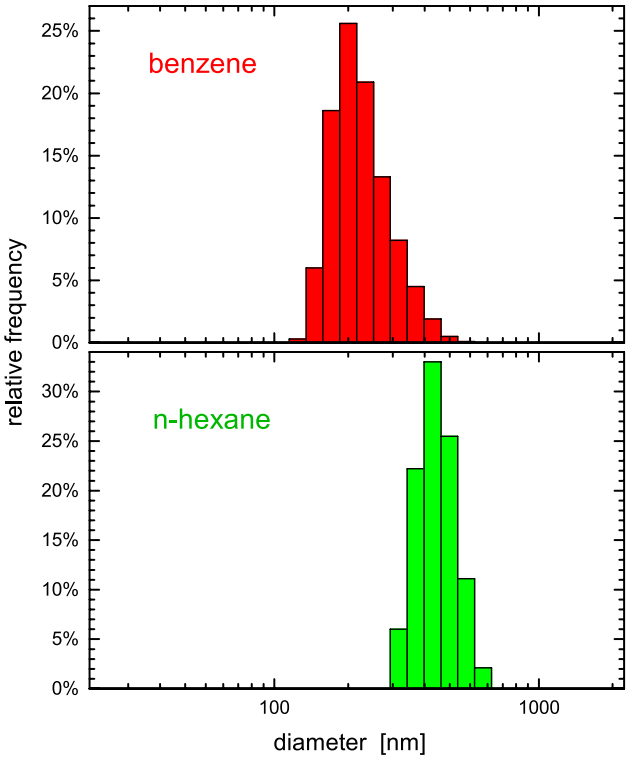

Fig. 6 Hydrodynamic diameters of the Epson toner material dissolved in benzene (top) and in n-hexane (bottom) obtained by DLS

with a range between 100 nm and 400 nm, whereas it is larger for particles dissolved in n-hexane with a mean value of about 450 nm and a range between 300 and 600 nm. In order to have access to the dispersity of the toner particles, the polydispersity index has additionally been determined. It amounts to 0.31 for toner particles dissolved in benzene and to 0.38 for particles dissolved in n-hexane. Both values are in the range of 0.1–0.4 which indicates an intermediate, moderately polydisperse distribution type where the distribution is neither extremely polydisperse, or broad, nor in any sense narrow.

3.2.3 XRD

The X-ray diffraction measurement is shown in Fig. 7. It is obvious that no sharp peaks occur. Therefore, the toner material does not exhibit any crystalline substances because the broad structures indicate the presence of disorder in the sample. The structures at around 20° and slightly above 40° hints generally to amorphous carbon [41, 42] like carbon black [43].

3.2.4 TEM

The TEM results show that agglomerates of several µm are present (see left part of Fig. 8). A detailed image of such

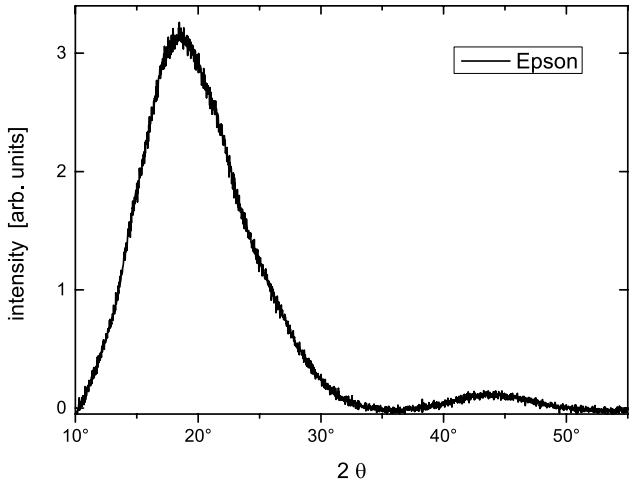

Fig. 7 X-ray diffraction pattern of the Epson toner material after background subtraction

an agglomerate proves (see right part of Fig. 8) that they are consisting of small nanoparticles. The determination of the respective diameters of about 25 particles results in (78 ± 6) nm.

3.2.5 SEM

The images taken with the SEM prove that large particles are present (see Fig. 9) with sizes between 5 and 15 µm. For the particle shown in the right part of the Figure, it can be seen that it is made up of smaller nanoparticles. This might be due to the preparation procedure because they were previously not dissolved as for the other characterization measurements which resulted in the break up of the agglomerates.

3.2.6 Conclusion

The chemical composition of the Epson toner material is only given by C and O. The hydrodynamic diameter of dissolved particles depends on the solvent and is at about 200 nm in benzene and around 450 nm in n-hexane. The size of the individual nanoparticles lies around 80 nm. They are completely amorphous, and no crystallization has taken place. The agglomeration of these nanoparticles results in agglomerates with sizes of about 10 µm.

3.3 Toner Lyreco

The content of the toner material is given in the data sheet with 43–53% styrene acrylate copolymer, 40–50% magnetite, below 1% metal complex dye, 1–5% ethylene propylene copolymer and below 3% silica.

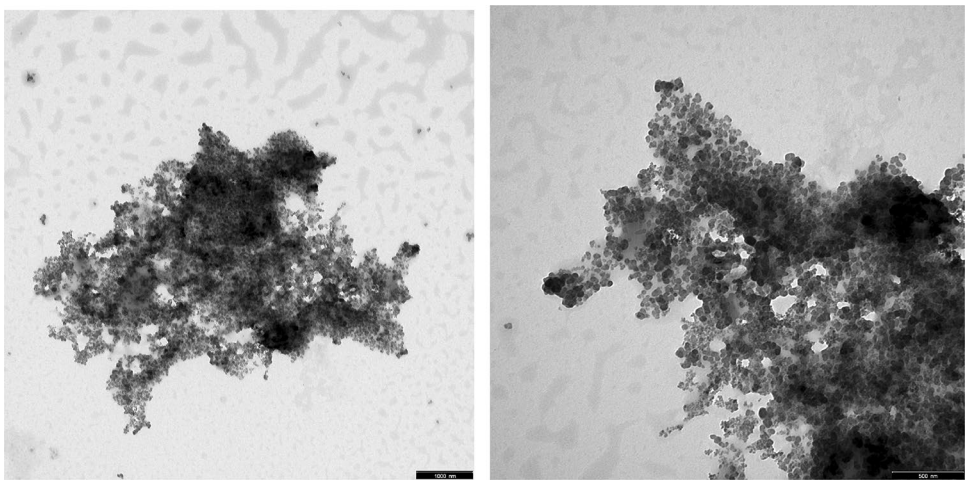

Fig. 8 TEM image of the Epson toner material after dissolving in benzene. Large agglomerates (left with a scale bar of 1000 nm) consist of individual nanoparticles (right with a scale bar of 500 nm)

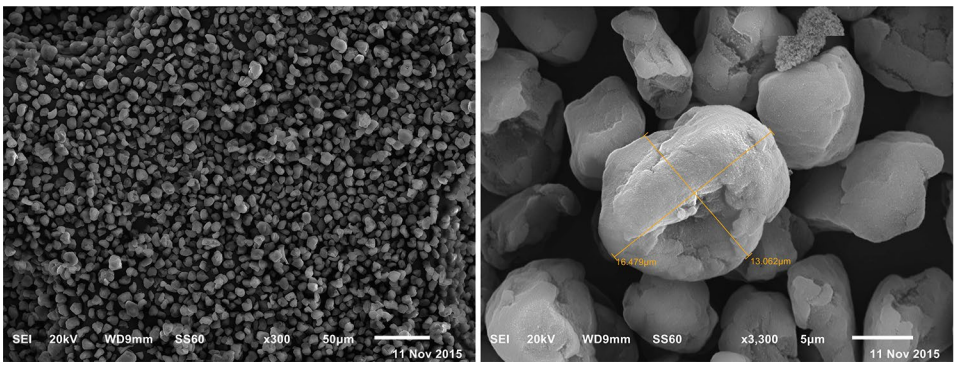

Fig. 9 SEM images of the Epson toner material with low (left part with a scale bar of 50 µm) and higher magnification (right part with a scale bar of 5 µm). The size of these particles is approximately between 5 and 15 µm

Table 3 Chemical composition of the Lyreco toner material obtained by EDX

Element	At. weight (%)	Uncertainty (%)
C	90.3	5.1
O	6.6	0.7
Si	0.5	0.1
Other	2.6	

3.3.1 EDX

EDX was used to determine the chemical composition. The significant relative amounts are listed in Table 3. It is striking that Fe as a part of magnetite is not detectable being in strong contrast to the declaration in the data sheet. The XRD measurements (see below) also prove that magnetite is not detectable in the toner material.

3.3.2 DLS

Dynamic light scattering measurements were carried out to determine the hydrodynamic diameter of the toner particles (see Fig. 10). The top diagram displays the sizes for toner material dissolved in benzene. Two different size regimes can be found with about 100 nm and around 400 nm. Dissolving the material in n-hexane (bottom diagram) one obtains a monomodal size distribution at around 70 nm. For the bimodal distribution (benzene as solvent), the polydispersity index is at about 0.5 which can be understood due to the two different sizes. For the monomodal distribution (n-hexane as solvent), the polydispersity index amounts to slightly below 0.8. This value hints to a relatively broad size distribution.

3.3.3 XRD

For the determination of crystalline material within the toner, X-ray diffraction measurements were used (see Fig. 11). The black curve displays the diffraction intensity of the Lyreco toner material. Tridymite and β-quartz (both different configurations of silica SiO_2) are the only materials which exhibit nearly the same diffraction peaks and are made up of the elements which were determined by EDX. The respective diffraction patterns are additionally given in Fig. 11. The red curve shows the pattern of tridymite, the

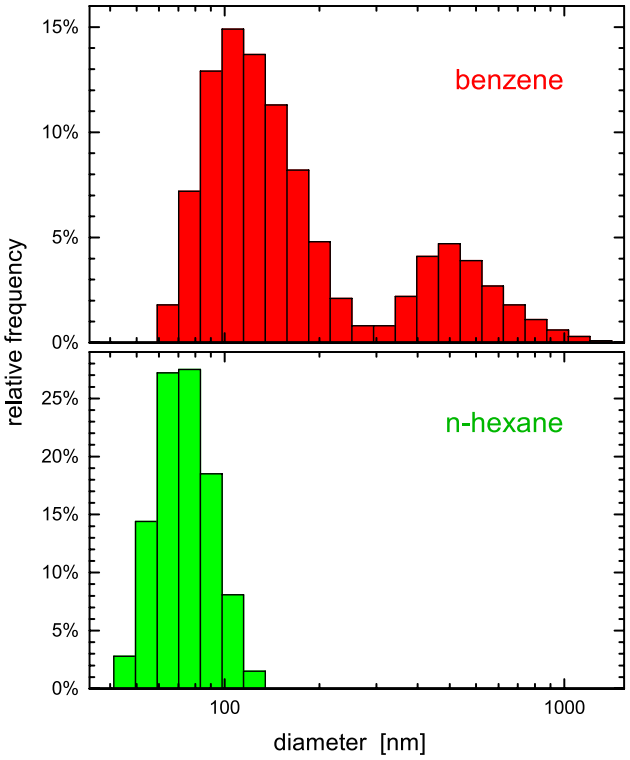

Fig. 10 Hydrodynamic diameter of Lyreco toner material obtained by DLS. Top: dissolved in benzene. Bottom: dissolved in n-hexane

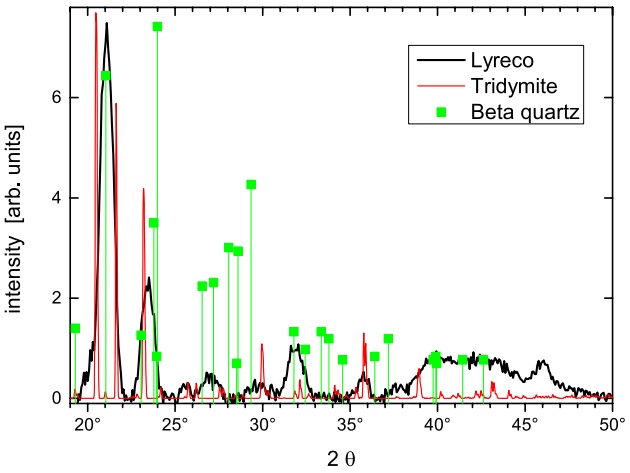

Fig. 11 X-ray diffraction pattern of the Lyreco toner material after background subtraction (black curve). Two reference diffractograms were additionally given with tridymite (red curve) and β -quartz (green dots) scaled to obtain the same maximum value

values were obtained from the RRUFF database (R090042). The green dots are values of β- or high-quartz [40].

As already found for the HP toner material (see Sect. 3.1.3) one alone cannot reproduce all pattern of the toner. The pattern at about 21° agrees with one of β -quartz, whereas tridymite exhibits two peaks at 20.5° and 21.5°. The peak at 23° can be reproduced with both materials, the one at 27° only with β-quartz, the peak at 36° only with tridymite. Therefore, the diffraction pattern hints to crystalline particles consisting of both types of silica. The broad structure between 38° and 48° can be understood as being due to β-quartz but is more likely due to amorphous carbon.

The two prominent peaks of the diffraction pattern are used to estimate the size of the crystalline particles using the Scherrer equation (see Eq. 2). The black dots represent the measurement of the toner material, the blue curve a fit with two Gaussian functions (see Fig. 12) which can reproduce the data very well. The fit results in an angle of $(21.1 \pm 0.1)°$ and a width (FWHM) of $(0.87 \pm 0.01)°$ for the first peak and an angle of $(23.4 \pm 0.1)°$ and a width of $(0.80 \pm 0.04)°$ for the second peak, resp. Using a Scherrer constant K of 0.94 which is taken for spherical particles with cubic symmetry, the obtained diameters amount to (9.7 ± 0.1) nm for the first and (10.6 ± 0.5) nm for the second peak.

3.3.4 TEM

The TEM image of toner material being dissolved in benzene is shown in Fig. 13. The large-scale view (left) demonstrates that most are located in a microscaled agglomeration but remain single objects. One can also recognize that few single particles are present. A rough estimation results in a size of about 100 nm. A detailed view with HR-TEM on single particles (right) proves a size of around 200 nm. These particles are made up of smaller ones with a size of about 50 nm. The chemical composition of these nanoparticles was additionally determined by EDX to be Si and O.

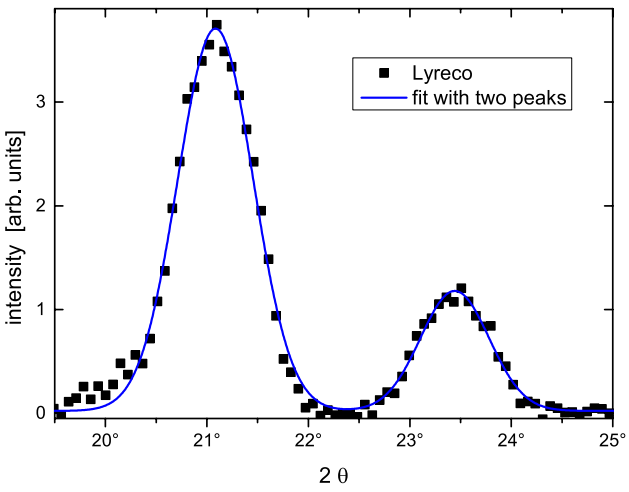

Fig. 12 X-ray diffraction pattern of Lyreco toner material in the angle range between 19.5° and 25° (black dots). Both peaks were fitted with two Gaussian functions (blue line)

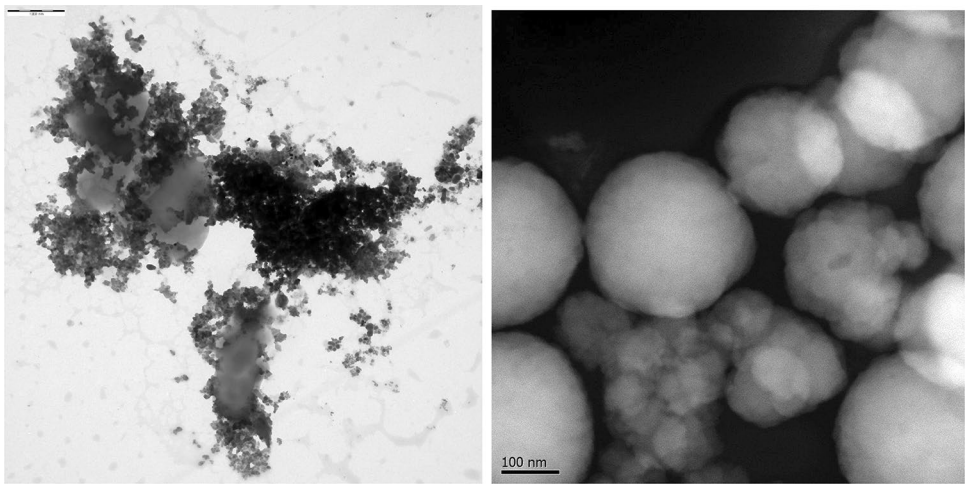

Fig. 13 TEM image of Lyreco toner material dissolved in benzene. Left: scale bar: 1000 nm. Right: scale bar: 100 nm

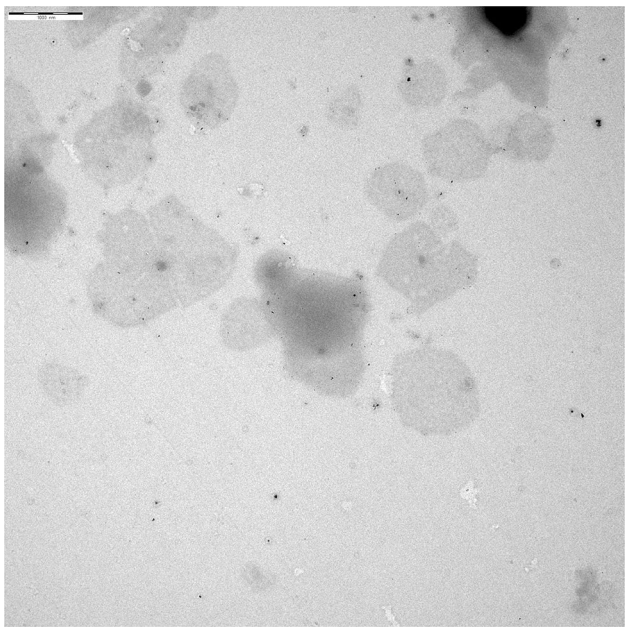

Fig. 14 TEM image of Lyreco toner material dissolved in n-hexane. The nanoparticles are seen as the small black dots. Scale bar: 1000 nm

The toner material was also dissolved in n-hexane. The corresponding TEM image is shown in Fig. 14. Being different from the dissolving in benzene, no agglomeration occurs. The toner particles remain as rather small single objects.

3.3.5 SEM

The behavior of the toner material without dissolving can be observed using SEM. Such an image is shown in Fig. 15. The small toner particles are found to be within large agglomerates with a size of several µm. They exhibit a nearly spherical shape.

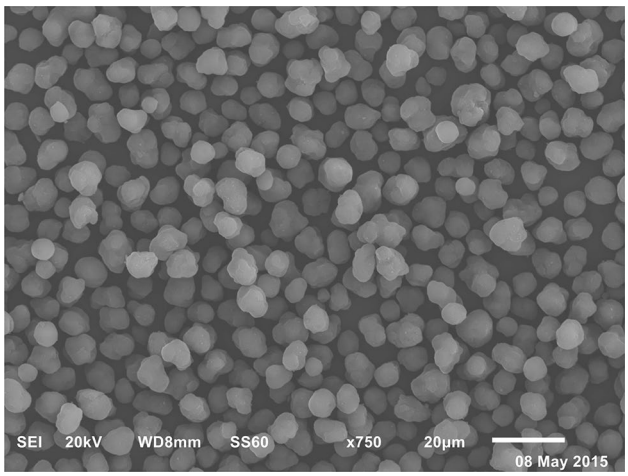

Fig. 15 SEM image of the Lyreco toner material without a previous dissolving

3.3.6 Conclusion

The chemical composition was determined with different experimental techniques all resulting in the same elements. EDX with SEM and also with HR-TEM as well as XRD proves the exclusive existence of C, O, and Si. This is in striking contrast to the data sheet which announces about 50% magnetite.

The toner material consists of large particles that are several µm in size in the undissolved powder. After dissolving the toner particles in benzene one gets micron-sized agglomerates consisting of nanoparticles. According to DLS, the agglomerates dissolved in benzene exhibit a bimodal size distribution of in average 100 nm and 400 nm. Using n-hexane as solvent, only smaller individual nanoparticles are present with a diameter of around 50 nm. The nanoparticles exhibit a crystalline core made up of silica with a diameter of about 10 nm

being determined due to the width of XRD diffraction peaks.

4 Discussion

All three toner materials (investigated by EDX) consist of C and O and with exception of the Epson toner of Si, too. No metallic content was observed although in one (Lyreco) 50% should be of magnetite as stated in the data sheet. The configuration could be determined by XRD. It was found that crystalline nanoparticles are present as SiO_2 (as β-quartz and tridymite) for the toners exhibiting Si. The size of the particles in the toner dust (i.e., without dissolution) is about 10 µm for all three toners. These particles are agglomerates of smaller particles.

Dissolving of the toner material in water was not possible. This can be understood as tridymite as well as quartz is practically unsolvable in this liquid [44]. Thus, nearly nonpolar solvents were chosen but with different properties in order to determine the dependence on the polarity. It was observed that dissolving the particles can be carried out with such a nonpolar solvent as shown for benzene and n-hexane (the solubility in water is about 10 mg/l for n-hexane and 1770 mg/l for benzene [44]). Being dissolved in benzene, the particles are made up of smaller agglomerates. The hydrodynamic diameter is monomodal with about 200 nm for HP and Epson and bimodal with about 100 nm and 400 nm for Lyreco.

They consist of nanoparticles with sizes being significantly different for the three toners. In the case of HP, they are approximately 20 nm and consist of crystalline SiO_2. For Lyreco, they are larger with about 200 nm exhibiting a crystalline core of about 10 nm made up of SiO_2. For Epson, they are amorphous carbon with a size of about 80 nm.

Using n-hexane as solvent, the small agglomerates for the HP toner exhibit a hydrodynamic diameter of about 50 nm which hints to single nanoparticles with a crystalline core of SiO_2 being about 20 nm covered with a ligand shell. A similar behavior was found for Lyreco. In this case, the occurrence of individual single nanoparticles could be proven by TEM. The small agglomerates of the Epson toner are significantly larger with about 500 nm consisting of amorphous carbon nanoparticles.

Therefore, cheap toner material can be used to obtain crystalline SiO_2 nanoparticles with a size of about 10–20 nm using the investigated toner material from HP and Lyreco. With benzene as solvent, they are agglomerated to particles of about 200–400 nm. Using n-hexane, one gets single nanoparticles without agglomeration. Additionally, amorphous carbon nanoparticles can be gained with a size of approximately 80 nm using the toner powder from Epson.

A further goal of this investigation was directed to possible differences between toner powders which are distributed by original equipment manufacturers to be used exclusively in their own printers and toners from general office supplies manufacturers to be used in many printer types which often offer recycled toner material. It was shown for the three specific toners that the properties of that from HP and Lyreco are rather similar, whereas large difference is present for the toner from Epson. Therefore, the origin seems not to play a prominent role.

Inhalation is the most significant exposure route for airborne particles [45–48]. Spherical solid material can be inhaled when its (in this case aerodynamic [49]) diameter is less than 10 µm. The smaller micron-sized particles are the deeper they can travel into the lung [45]. Particles smaller than 2.5 µm will even reach the alveoli [46].

The lung consists of two functional parts, the airways (with the two sections of the nasal, pharyngeal and laryngeal region on the one hand and the tracheobronchial region consisting of the trachea, bronchi and bronchioles on the other hand both responsible for transporting the air in and out the lungs) and the alveolar region (as gas exchange areas).

In each of the three regions of the respiratory tract, significant amounts of a certain size of particles are deposited after inhalation [47]. 90% of inhaled particles with a diameter of 1 nm are deposited in the nasopharyngeal compartment, only 10% in the tracheobronchial region and essentially none in the alveolar region. Contrarily, particles with a diameter of 5 nm exhibit about equal deposition of approximately 30% of the inhaled particles in all three regions. Particles with a diameter of 20 nm have the highest deposition efficiency in the alveolar region with about 50%, whereas in the nasopharyngeal and tracheobronchial regions, this particle size deposits with about 15% efficiency.

These distributions are for particles which are inhaled as individual, single objects of a given size and not as agglomerates. The latter exhibit obviously larger particle sizes and therefore different deposition sites.

For all three toner materials, the particles without dissolving show a diameter of about 10 µm. Silica particles are insoluble in water and remain therefore unaffected, i.e., without changing their size after inhalation. This is important because they are of particular toxicological relevance below about 5 µm [44]. Thus, most of these particles should remain in the nasopharyngeal region without reaching the alveolar region [45]. The clearance of micron-sized particles from this region is carried out by mucociliary clearance which means by the movement of cilia and the mucous layer.

In the case of a possible dissolution in a nonpolar solvent, the now nanoparticles should exhibit a different

behavior for the distribution to the three regions because they have different sizes depending on the manufacturer. That means that they can reach the alveolar region which is of importance from a toxicological point of view. Additionally, it was shown that the solvent itself has a significant influence on the size and size distribution even for the same toner powder.

As a general consideration, this investigation may be helpful to give more information concerning possible health hazards due to the use of printers and copiers which emit particle dust coming from the toner because only little quantitative information is available for the characterization concerning the size and chemical composition of the particulate matter emitted by office equipment and a toxicological assessment of the emitted particles requires the knowledge of their chemical composition. In particular, former investigations are carried out in dependence of printer or copier types but not of possible toners which are made up of different content. The use of different toners may be the explanation why in investigations of printers not only from different manufacturers but also for identically constructed devices often significant differences in the behavior of emitted nanoparticles are present.

5 Summary

Printer toner is a material in everyday life. It is a cheap material which is distributed by many companies. Each printer and copier require specific toner material. Therefore, differences in the consistence occur concerning the size and chemical composition of the toner particles. They are known as microscaled objects which are made up of nanoparticles.

The first goal of this investigation was to determine the material composition as well as the size, the shape and the possible crystallinity of the particles from three different toner materials (distributed by Hewlett-Packard, Lyreco and Epson) to turn one's attention whether these nanoparticles can be taken for scientific investigations instead of carrying out sophisticated preparation procedures as well as to use them for teaching purpose or for practical training.

It was found that cheap toner material can be used to obtain crystalline SiO_2 nanoparticles with a size of about 10–20 nm using the investigated toner material from HP and Lyreco. With benzene as solvent, they are agglomerated to particles of about 200–400 nm. Using n-hexane, one gets single nanoparticles without agglomeration. Additionally, amorphous carbon nanoparticles can be gained with a size of approximately 80 nm using the toner powder from Epson.

A second goal of this investigation was directed to possible differences between toner powders which are distributed by original equipment manufacturers to be used exclusively in their own printers and toners from general office supplies manufacturers to be used in many printer types which often offer recycled toner material. It was shown for the three specific toners that the properties of that from HP and Lyreco are rather similar, whereas large difference is present for the toner from Epson. Therefore, it seems not to play a significant role whether the toner is obtained from original equipment or general office supplies manufacturers.

A third goal was directed to give more information concerning possible health hazards due to the use of printers and copiers which emit particle dust coming from the toner. Due to that particulate pollution inspiration can result in inflammatory processes in the lung up to lung cancer. Additionally, nanoparticles can have a toxic effect within cells and be mutagenic. For all three toner materials, the particles without dissolving show a diameter of about 10 µm. Therefore, most of these particles should remain in the nasopharyngeal region without reaching the alveolar region. In the case of dissolution the now nanoparticles should exhibit different behavior for the distribution to the three regions because they have different sizes depending on the manufacturer. Additionally, it was shown that the solvent itself has a significant influence on the size and size distribution even for the same toner powder.

Acknowledgements Taking the TEM images was done by Marion Nissen (Center of Advanced Imaging CAi at the University of Düsseldorf) and the HR-TEM images by Martina Pohl (University of Rostock) which is gratefully acknowledged. Additionally, we thank Karsten Klauke (Univ. Düsseldorf) for some PXRD measurements and Dennis Dietrich (Univ. Düsseldorf) for SEM/EDX investigations.

Compliance with ethical standards

Conflict of interest On behalf of all authors, the corresponding author states that there is no conflict of interest.

References

1. Koivisto AJ, Hussein T, Niemelä R, Tuomi T, Hämeri K (2010) Impact of particle emissions of new laser printers on modeled office room. Atmos Environ 44:2140
2. Baker SH, Thornton SC, Edmonds KW, Maher MJ, Norris C, Binns C (2000) The construction of a gas aggregation source for the preparation of size-selected nanoscale transition metal clusters. Rev Sci Instrum 71:3178
3. Methling RP, Senz V, Klinkenberg ED, Diederich Th, Tiggesbäumker J, Holzhüter G, Bansmann J, Meiwes-Broer KH (2001) Magnetic studies on mass-selected iron particles. Eur Phys J D 16:173
4. Haberland H, Karrais M, Mall M, Thurner Y (1992) Thin films from energetic cluster impact: a feasibility study. J Vac Sci Technol A 10:3266

5. Binns C (2001) Nanoclusters deposited on surfaces. Surf Sci Rep 44:1
6. de Heer WA (1993) The physics of simple metal clusters: experimental aspects and simple models. Rev Mod Phys 65:611
7. Bansmann J, Baker SH, Binns C, Blackman JA, Bucher JP, Dorantes-Davila J, Dupuis V, Favre L, Kechrakos D, Kleibert A, Meiwes-Broer K-H, Pastor GM, Perez A, Toulemonde O, Trohidou KN, Tuaillon J, Xie Y (2005) Magnetic and structural properties of isolated and assembled clusters. Surf Sci Rep 56:189
8. Sun S, Murray CB, Weller D, Folks L, Moser A (2001) Monodisperse FePt nanoparticles and ferromagnetic FePt nanocrystal superlattices. Science 287:1989
9. Mittleman DM, Schoenlein RW, Shiang JJ, Colvin VL, Alivisatos AP, Shank CV (1994) Quantum size dependence of femtosecond electronic dephasing and vibrational dynamics in CdSe nanocrystals. Phys Rev B 49:14435
10. Link St, El-Sayed MA (1999) Spectral properties and relaxation dynamics of surface plasmon electronic oscillations in gold and silver nanodots and and nanorods. J Phys Chem B 103:8410
11. Bailey RE, Smith AM, Nie S (1985) Quantum dots in biology and medicine. Physica E 25:1
12. Knickelbein MB, Yang S, Riley St J (1990) Near-threshold photoionization of nickel clusters: ionization potentials for Ni_3 to Ni_{90}. J Chem Phys 93:94
13. Leuchtner RE, Harms AC, Castleman AW (1989) Thermal metal cluster anion reactions: behavior of aluminum clusters with oxygen. J Chem Phys 91:2753
14. Billas IML, Châtelain A, de Heer WA (1994) Magnetism from the atom to the bulk in iron, cobalt, and nickel clusters. Science 265:1682
15. Buffat Ph, Borel JP (1976) Size effect on the melting temperature of gold particles. Phys Rev A 13:2287
16. Wang Z-M, Wagner J, Wall St (2011) Characterization of laser printer nanoparticle and VOC emissions, formation mechanisms, and strategies to reduce airborne exposures. Aerosol Sci Technol 45:1060
17. Lee SC, Lam S, Fai HK (2001) Characterization of VOCs, ozone, and PM_{10} emissions from office equipment in an environmental chamber. Build Environ 36:837
18. Kagi N, Fujii S, Horiba Y, Namiki N, Ohtani Y, Emi H, Tamura H, Kim YS (2007) Indoor air quality for chemical and ultrafine particle contaminants from printers. Build Environ 42:1949
19. He C, Morawska L, Taplin L (2007) Particle emission characteristics of office printers. Environ Sci Technol 41:6039
20. Tang T, Hurraß J, Gminski M, Mersch-Sundermann V (2012) Fine and ultrafine particles emitted from laser printers as indoor air contaminants in German offices. Environ Sci Pollut Res 19:3840
21. Cheng YS, Yamada Y, Yeh HC, Swift DL (1990) Deposition of ultrafine aerosols in a human oral cast. Aerosol Sci Technol 12:1075
22. Peters A, Wichmann HE, Tuch T, Heinrich J, Heyder J (1997) Respiratory effects are associated with the number of ultrafine particles. Am J Respir Crit Care Med 155:1376
23. Donaldson K, Tran L, Jimenez LA, Duffin R, Newby DE, Mills N, MacNee W, Stone V (2005) Combustion-derived nanoparticles: a review of their toxicology following inhalation exposure. Part Fibre Toxicol 2:10
24. Veranth JM, Ghandehari H, Grainger DW (2010) Nanoparticles in the lung. Compr Toxicol 8:453
25. Tang T, Gminski R, Könczöl M, Modest Ch, Armbruster B, Mersch-Sundermann V (2012) Investigations on cytotoxic and genotoxic effects of laser printer emissions in human epithelial A549 lung cells using an air/liquid exposure system. Environ Mol Mutagen 53:125
26. Könczöl M, Weiß A, Gminski R, Merfort I, Mersch-Sundermann V (2013) Oxidative stress and inflammatory response to printer toner particles in human epithelial A549 lung cells. Toxicol Lett 216:171
27. Chang LY, Crapo JD, Gehr P, Rothen-Rutishauser B, Mühfeld C, Blank F (2018) Alveolar epithelium in lung toxicology. Compr Toxicol 15:50
28. Bierkandt FS, Leibrock L, Wagener S, Laux P, Luch A (2018) The impact of nanomaterial characteristics on inhalation toxicity. Toxicol Res 7:321
29. Iavicoli I, Leso V, Schulte PA (2016) Biomarkers of susceptibility: state of the art and implications for occupational exposure to engineered nanomaterials. Toxicol Appl Pharmacol 299:112
30. Lu X, Miousse IR, Pirela SV, Melnyk S, Koturbash I, Demokritou Ph (2016) Short-term exposure to engineered nanomaterials affects cellular epigenome. Nanotoxicology 10:140
31. Pirela SV, Miousse IR, Lu X, Castranova V, Thomas T, Qian Y, Bello D, Kobzik L, Koturbash I, Demokritou Ph (2016) Effects of laser printer-emitted engineered nanoparticles on cytotoxicity, chemokine expression, reactive oxygen species, DNA methylation, and DNA damage: A comprehensive in-vitro analysis in human small airway epithelial cells, macrophages, and lymphoblasts. Environ Health Perspect 124:210
32. Destaillats H, Maddalena RL, Singer BC, Hodgson AT, McKone TE (2008) Indoor pollutants emitted by office equipment: a review of reported data and information needs. Atmos Environ 42:1371
33. Barthel M, Pedan V, Hahn O, Rothhardt M, Bresch H, Jann O, Seeger St (2011) XRF-analysis of fine and ultrafine particles emitted from laser printer devices. Environ Sci Technol 45:7819
34. Wensing M, Schripp T, Uhde E, Salthammer T (2008) Ultra-fine particles release from hardcopy devices: sources, real-room measurements and efficiency of filter accessories. Sci Total Environ 407:418
35. Pirela SV, Pyrgiotakis G, Bello D, Thomas T, Castranova V, Demokritou Ph (2014) Development and characterization of an exposire platform suitable for physico-chemical, morphological and toxicological characterization of printer-emitted particles. Inhal Toxicol 26:400
36. Morawska L, He C, Johnson G, Jayaratne R, Salthammer T, Wang H, Uhde E, Bostrom Th, Modini R, Ayoko G, McGarry P, Wensing M (2009) An investigation into the characteristics and formation mechanisms of particles originating from the operation of laser printers. Environ Sci Technol 43:1015
37. He C, Morawska L, Wang H, Jayaratne R, McGarry P, Johnson GR, Bostrom Th, Gonthier J, Authemayou St, Ayoko G (2010) Quantification of the relationship between fuser roller temperature and laser printer emissions. J Aerosol Sci 41:523
38. Wang D, Guo H, He C (2017) An investigation on particle emission from a new laser printer using an environmental chamber. Indoor Built Environ 26:1144
39. Holzwarth U, Gibson N (2011) The Scherrer equation versus the Debye-Scherrer equation. Nat Nanotechnol 6:534
40. Wright AF, Lehmann MS (1981) The structure of quartz at 25 and 590°C determined by neutron diffraction. J Solid State Chem 36:371
41. Klug HP, Alexander LE (1974) X-ray diffraction procedures for polycrystalline and amorphous materials, 2nd edn. Wiley, London
42. Lazzarini A, Piovano A, Pellegrini R, Agostini G, Rudic S, Lamberti C, Groppo E (2016) Graphitization of activated carbons: a molecular-level investigation by INS, DRIFT, XRD and Raman techniques. Phys Proc 85:20
43. Xie X, Liu J, Li T, Song Y, Wang F (2018) Post-formation copper-nitrogen species on carbon black: their chemical structures and active sites for oxygen reduction reaction. Chem Eur J 24:9968
44. GESTIS Substance database: gestis-en.itrust.de with following numbers (quartz 004110, tridymite 570262, benzene 010060, n-hexane 510789)

45. Byron PR (1986) Prediction of drug residence times in regions of the human respiratory tract following aerosol inhalation. J Pharm Sci 75:433
46. Hoet PHM, Brüske-Hohlfeld I, Salata OV (2004) Nanoparticles—known and unknown health risks. J Nanobiotechnol 2:12
47. Oberdörster G, Oberdörster E, Oberdörster J (2005) Nanotoxicology: an emerging discipline evolving from studies of ultrafine particles. Environ Health Perspect 113:823
48. Yang W, Peters JI, Williams RO (2008) Inhaled nanoparticles—a current review. Int J Pharm 356:239
49. DeCarlo PF, Slowik JG, Worsnop DR, Davidovits P, Jimenez JL (2004) Particle morphology and density characterization by combined mobility and aerodynamic diameter measurements. Part 1: theory. Aerosol Sci Technol 38:1185